Hypervariable Domain of Nonstructural Protein nsP3 of Venezuelan Equine Encephalitis Virus Determines Cell-Specific Mode of Virus Replication

Niall J. Foy, Maryna Akhrymuk, Alexander V. Shustov, Elena I. Frolova, Ilya Frolov

Department of Microbiology, University of Alabama, Birmingham, Alabama, USA

Venezuelan equine encephalitis virus (VEEV) is one of the most pathogenic members of the *Alphavirus* genus in the *Togaviridae* family. This genus is divided into the Old World and New World alphaviruses, which demonstrate profound differences in pathogenesis, replication, and virus-host interactions. VEEV is a representative member of the New World alphaviruses. The biology of this virus is still insufficiently understood, particularly the function of its nonstructural proteins in RNA replication and modification of the intracellular environment. One of these nonstructural proteins, nsP3, contains a hypervariable domain (HVD), which demonstrates very low overall similarity between different alphaviruses, suggesting the possibility of its function in virus adaptation to different hosts and vectors. The results of our study demonstrate the following. (i) Phosphorylation of the VEEV nsP3-specific HVD does not play a critical role in virus replication in cells of vertebrate origin but is important for virus replication in mosquito cells. (ii) The VEEV HVD is not required for viral RNA replication in the highly permissive BHK-21 cell line. In fact, it can be either completely deleted or replaced by a heterologous protein sequence. These variants require only one or two additional adaptive mutations in nsP3 and/or nsP2 proteins to achieve an efficiently replicating phenotype. (iii) However, the carboxy-terminal repeat in the VEEV HVD is indispensable for VEEV replication in the cell lines other than BHK-21 and plays a critical role in formation of VEEV-specific cytoplasmic protein complexes. Natural VEEV variants retain at least one of the repeated elements in their nsP3 HVDs.

The *Alphavirus* genus in the *Togaviridae* family contains a number of human and animal pathogens (1). Under natural conditions, alphaviruses circulate between mosquito vectors and vertebrate hosts (2). In mosquitoes, they cause a persistent, life-long infection and accumulate to high titers in salivary glands. This concentration of viral particles in the saliva leads to virus transmission to vertebrates during the next blood meal. In mammalian and other hosts, alphaviruses induce high-titer viremia, which is required for transmission of the virus to new mosquito vectors (3). Some of the alphaviruses, such as Venezuelan equine encephalitis virus (VEEV), eastern equine encephalitis virus (EEEV), and western equine encephalitis virus (WEEV), are capable of causing severe meningoencephalitis with frequently lethal outcomes, not only in small animals and birds but also in humans and equids (2). Others, such as Ross River virus, o'nyong nyong virus, chikungunya virus (CHIKV), and Sindbis virus (SINV), cause less severe disease, characterized by rash, arthritis, and fever (4). Continuous circulation of alphaviruses on all continents and their ability to cause diseases of different severities in humans make them a significant public health threat. Moreover, a recent outbreak of CHIKV with millions of people infected and the ability of this virus to develop a severe disease strongly indicate that the importance of alphaviruses as human pathogens is quite underappreciated (5–8). To date, no efficient therapeutic means against any alphavirus infection have been developed, primarily due to our insufficient knowledge of the molecular mechanism of virus replication and their interactions with the hosts.

The alphavirus genome is represented by a single-stranded, 11.5-kb RNA of positive polarity (9). It mimics the structure of cellular mRNA templates, in that it has a cap at the 5′ terminus and a poly(A) tail at the 3′ terminus. This RNA encodes only a few proteins. Four nonstructural proteins, nsP1 to nsP4, are translated as P123 and P1234 polyproteins directly from the genomic RNA after its release from the nucleocapsid to the cytoplasm. Together with host protein factors (10–14), partially or completely processed nsPs form replication enzyme complexes synthesizing negative-strand RNA genome intermediates, positive-strand genomes, and subgenomic RNA. The subgenomic RNA serves as a template for translation of viral structural proteins, capsid, and glycoproteins E2 and E1, which ultimately interact to form viral particles (3). Functions of the structural proteins in viral particle formation are reasonably well understood (15), but the mechanism of the nsPs' function in viral RNA synthesis and virus-host cell interactions remains poorly studied. At this point, we know that the initially synthesized P123 and P1234 polyproteins are sequentially processed into individual nsP1, nsP2, nsP3, and nsP4 by nsP2-associated protease activity, and this processing regulates the specificity of the replication complex in the synthesis of different virus-specific RNAs (16). The initially formed P123- and nsP4-containing complexes can synthesize the negative-strand RNA in a double-stranded RNA (dsRNA) intermediate form. After complete processing, nsP1 to nsP4 form mature replication complexes, which are active in the synthesis of both the viral genome and subgenomic RNAs but no longer synthesize the negative-strand RNA (17, 18). In these complexes, nsP1 accomplishes most of the RNA-capping functions (19). nsP2 demonstrates

NTPase, RTPase, and RNA helicase activities (20–23). The roles of its amino-terminal, protease, and S-adenosylmethionine (SAM)-methyltransferase-like domains in complex formation and RNA synthesis remain to be further determined (23–26). nsP4 is an RNA-dependent RNA polymerase, and it also appears to be directly involved in recognition of the promoters on the negative-strand RNA intermediate (27, 28). To date, no defined functions have been assigned to the nsP3 protein. Information about nsP3 activities in viral replication is quite limited. However, it has been shown that some mutations in the nsP3 gene differentially affect synthesis of alphavirus-specific RNAs and can have deleterious effects on virus replication (29, 30). In SINV-infected cells, nsP3 was found to form at least two types of complexes with distinct protein contents and functions (14). It was also demonstrated that alphavirus nsP3 contains two conserved domains and a hypervariable domain (HVD), which is characterized by a lack of defined folding and appears to be strongly phosphorylated (29, 31, 32). Compared to other nsPs, nsP3 and its HVD in particular demonstrate low levels of identity between the members of the alphavirus genus (31). Efforts to analyze the crystal structure of nsP3 have been partially successful. Crystal structures of more conserved amino-terminal nsP3 domains (macro domains) of VEEV and CHIKV and a fragment of SINV nsP2 followed by the conserved domain of nsP3 were solved (33, 34). The macro domain was found to exhibit a high level of similarity with the ADP-ribose 1″-phosphate phosphatases in terms of protein folding (33, 35). In biochemical tests, it demonstrated some activities characteristic of the human homologs of the enzyme (33). It was also proposed that the macro domain is involved in processing of Semliki Forest virus (SFV)-specific P23 (36). The role of the second conserved nsP3 domain, located between the macro domain and the HVD, also remains to be understood.

The alphavirus nsP3-specific HVD appears to be the most poorly understood protein fragment in terms of its function in virus replication. On one hand, it demonstrates a lack of conservation between alphaviruses belonging to different serocomplexes and a considerable diversity between the members of the same serocomplex. On the other hand, all the alphaviruses contain such a domain in nsP3, suggesting that it plays an essential role in virus replication.

In this study, we used a combination of reverse genetics and selection approaches to further analyze the function of nsP3 in the replication of one of the most pathogenic members of the genus, VEEV. Our data demonstrate that similarly to other alphavirus structural and nonstructural proteins, VEEV nsP3 has numerous functions in virus replication. The VEEV HVD was found to be nonessential for virus replication in highly permissive BHK-21 cells. A small number of adaptive point mutations was sufficient for restoring replication of VEEV mutants having the HVD replaced by a heterologous amino acid sequence or having the entire nsP3 HVD deleted. However, replication of VEEV in other cell types required the preservation of a unique repeating amino acid sequence in the carboxy terminus of the HVD, and the presence of at least one of the repeats rendered the virus capable of replication to high titers.

MATERIALS AND METHODS

Cell cultures. BHK-21 cells were kindly provided by Paul Olivo (Washington University, St. Louis, MO). NIH 3T3 cells were obtained from the American Type Culture Collection (Manassas, VA). These cell lines were maintained at 37°C in alpha minimum essential medium (αMEM) supplemented with 10% fetal bovine serum (FBS) and vitamins. Mosquito C7/10 cells were kindly provided by Henry Huang (Washington University, St. Louis, MO). These cells were maintained at 30°C in Dulbecco's modified Eagle's medium (DMEM) supplemented with 10% heat-inactivated FBS and 10% tryptose phosphate broth (TPB).

Plasmid constructs. A plasmid harboring the original VEEV genome, pVEEV/GFP, was described previously (37). This plasmid contained cDNA of the VEEV TC-83 genome, which also harbored the green fluorescent protein (GFP) gene under the control of the subgenomic promoter. This plasmid was used for modifications of the nsP3-encoding sequence using PCR-based techniques. The schemes of recombinant viral genomes, the critical sequences, and introduced mutations are presented in the relevant figures. All of the sequences and details of the cloning procedures can be provided upon request.

RNA transcriptions. Plasmids were purified by centrifugation in CsCl gradients. They were linearized by using the MluI restriction site located downstream of the poly(A) sequence of the cDNA of viral genomes. RNAs were synthesized by SP6 RNA polymerase in the presence of a cap analog under conditions described previously (38). The yield and integrity of transcripts were analyzed by gel electrophoresis under nondenaturing conditions, and transcription mixtures were used for electroporation without additional purification (39). Standard electroporations were performed by using 1 μg of the *in vitro*-synthesized RNA. Released viruses were harvested at 24 h postelectroporation, and titers were determined by a plaque assay on BHK-21 cells (40).

For most of the electroporations, to assess RNA infectivity and test whether virus replication required adaptive mutations in viral genes, we also performed an infectious center assay. For this assay, different numbers of electroporated cells were seeded onto monolayers of naive BHK-21 cells and, after 1 h of incubation at 37°C, covered by 0.5% agarose supplemented with media and 3% FBS. Depending on the ability of mutant viruses to spread and cause a cytopathic effect (CPE), either plaques were stained with crystal violet at 48 h postelectroporation or numbers of GFP-positive foci were measured by using a fluorescence microscope. Thus, RNA infectivity was measured in either PFU or focus-forming units (FFU) per microgram of RNA.

Viral replication analysis. Many of the mutants designed in this study demonstrated rapid evolution to a more efficiently replicating phenotype, and this strongly complicated the analysis of the originally designed constructs. Therefore, most of the analyses of virus replication efficiencies were performed directly on RNA-electroporated cells. One-fifth of the electroporated cells (see above) were seeded into 35-mm dishes, and media were replaced at the time points indicated in the figures. In other experiments, naive cells were seeded into 35-mm dishes. After a 4-h-long incubation at 37°C, monolayers were infected at the multiplicities of infection (MOIs) indicated in the figures or figure legends, washed with phosphate-buffered saline (PBS), and overlaid with 1 ml of complete medium. At the times indicated in the figures, media were replaced by fresh media, and virus titers were determined by a plaque assay on BHK-21 cells, as previously described (40).

Immunofluorescence analysis. For confocal microscopy, cells were seeded onto 8-well μ-slides (Ibidi GmbH, Munich, Germany), infected at an MOI of ca. 20 PFU/cell, and incubated at 37°C in a CO_2 incubator. At the indicated times, the cells were fixed in 4% paraformaldehyde (PFA) in PBS for 20 min at room temperature, permeabilized, and blocked with PBS supplemented with 0.5% Triton X-100–5% goat serum for 30 min. The cells were then stained with mouse monoclonal antibodies (MAbs) specific to VEEV nsP3, which were described previously (41), and secondary goat anti-mouse antibodies labeled with Alexa Fluor 555 (Invitrogen). Hoechst 34580 (Invitrogen) was used for staining of nuclei. Images were acquired on a Zeiss LSM700 confocal microscope with a 63×, 1.4-numerical-aperture (NA) PlanApochromat oil objective. Each image represents multiple-intensity projections of 6 optical sections.

A)

```
331              VEEV nsP3 HVD
VETPPVDETPEPSAENQSTEGTPEQPPLITEDETRTRTPEPIIIEEEEED
--G-----G---G----AG--G-------A---G-A-G------------

SISLLSDGPTHQVLQVEADIHGPPSVSSSSWSIPHASDFDVDSLSILDTL
A-G--G---A--------------G-AGAG-E----G-----N-G---A-

EGASVTSGATSAETNSYFAKSMEFLARPVPAPRTVFRNPPHPAPRTRTPS
---G-GA--GG--E-G----A------------G-----------G-A-G

LAPSRACSRTSLVSTPPGVNRVITREELEALTPSRTPSRSVSRTSLVSNP
---A---G-AG--AG--------G-------G-A-G-A-G-G-GG--A--

PGVNRVITREEFEAFVAQQQ       wt HVD
-------A------------       ST⁻HVD
                550
```

B)


```
                                        RNA Infectivity
                                           PFU/µg
VEEV/GFP
[nsP1][nsP2][ nsP3 HV ][nsP4]→[GFP][C][E2][E1]  9x10⁵

VEEV/ST⁻HVD/GFP
[nsP1][nsP2][ nsP3 HV ][nsP4]→[GFP][C][E2][E1]  2x10⁵
```

C)

BHK-21

- ● VEEV/ST⁻HVD/GFP
- ■ VEEV/GFP

D)
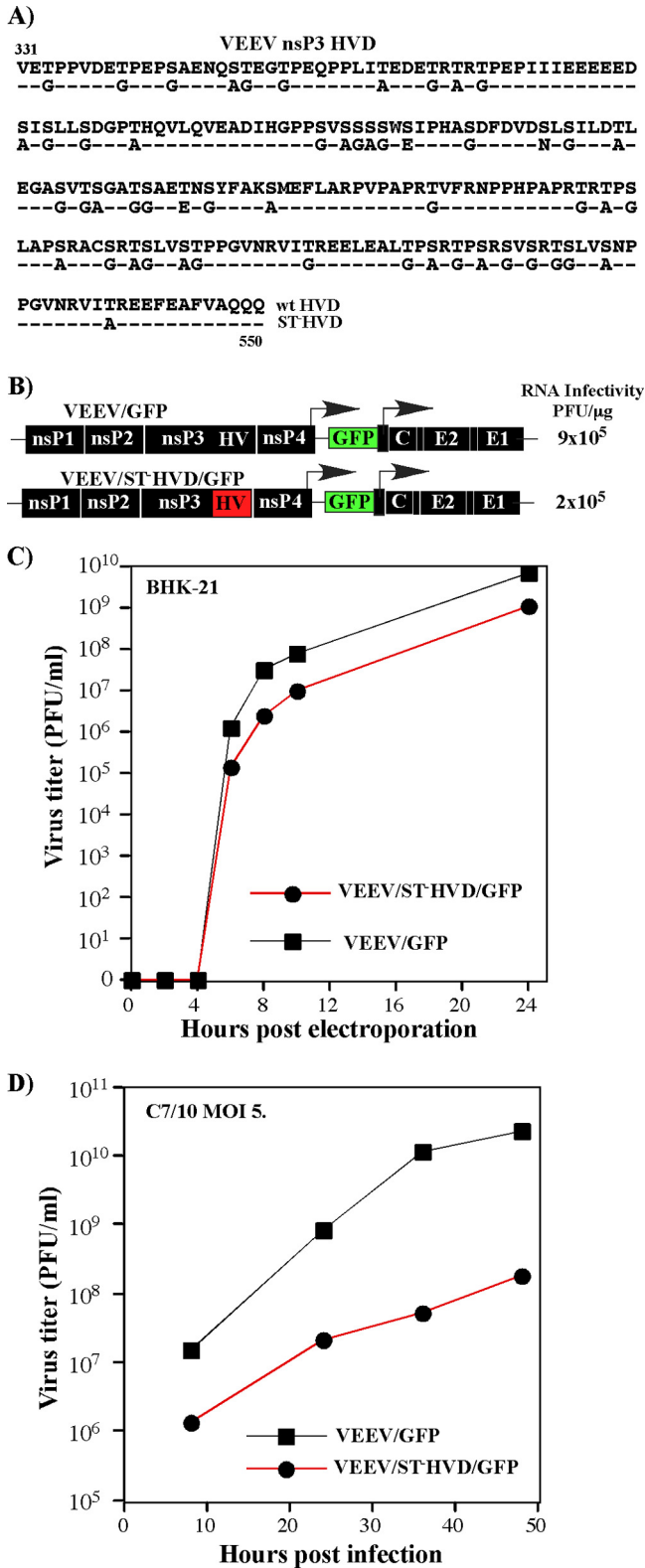

C7/10 MOI 5.

- ■ VEEV/GFP
- ● VEEV/ST⁻HVD/GFP

FIG 1 VEEV can tolerate mutations of all of the Ser and Thr residues in the HVD of nsP3. (A) Amino acid sequences of the VEEV-specific HVD and its mutated ST⁻ variant. (B) Schematic representation of the recombinant VEEV/ST⁻HVD/GFP and control VEEV/GFP virus genomes and infectivities of the *in vitro*-synthesized RNAs in the infectious center assay. (C) Replication of VEEV/ST⁻HVD/GFP and VEEV/GFP in BHK-21 cells after electroporation of

RESULTS

Modification of all potential phosphorylation sites in the VEEV nsP3 HVD affects virus replication in mosquito, but not BHK-21, cells. Our study was aimed at a further understanding of the function(s) of nsP3, and the HVD in particular, in VEEV replication. Alphavirus nsP3-specific HVDs demonstrate a very high level of evolution, and almost no homology in the amino acid sequences of this fragment between different members of the alphavirus genus has been found (41). Another characteristic feature of the nsP3-specific HVD is an unusually high percentage of Thr and Ser, which were proposed to represent a substrate for the previously described abundant nsP3 phosphorylation (31, 32, 42, 43). Functional significance of phosphorylation sites can be determined by sequential introduction of point mutations or making small deletions in the fragments of interest, followed by analysis of the virus phenotype. The VEEV nsP3-specific HVD contains 53 potential phosphorylation sites with possible redundant functions. Therefore, application of the first, point mutation-based approach is not feasible. The results of deletion analysis might be difficult to interpret because of the possible effect of deletion-induced changes on the overall protein folding and function. To at least partially avoid these problems, we replaced all of the 53 Ser- and Thr-specific codons in the nsP3 HVD-encoding sequence of the VEEV TC-83 genome (Fig. 1A) by those encoding Gly, Ala, Glu, and Gln and tested the effect of this extensive protein modification on virus replication. The choice of amino acid used was based on the attempt to save the hydrophilic profile of the HVD. Based on our previous experience, virus nonstructural polyprotein mutants can become noncytopathic and incapable of forming plaques (37, 44–46). Therefore, in these and most of our other experiments, we used viruses encoding GFP under the control of a subgenomic promoter. Thus, we could control virus viability and monitor their replication and spread by evaluating GFP expression in the monolayer of infected cells. The designed VEEV/ST⁻HVD/GFP genome, encoding the mutated nsP3, is presented in Fig. 1B.

Equal amounts of the *in vitro*-synthesized RNAs of VEEV/ST⁻HVD/GFP and the VEEV/GFP control (Fig. 1B) were electroporated into BHK-21 cells. We compared RNA infectivity by the infectious center assay and also analyzed the rates of virus replication (Fig. 1B and C). The introduction of 53 amino acid (aa) substitutions did not affect the RNA infectivity. The small differences observed remained within the limits of accepted variations between the experiments. This suggested that for at least the initiation of replication, no additional, adaptive mutations were required. Fifty-three mutations had a detectable but minor effect on the rate of virus replication in BHK-21 cells (Fig. 1C). The VEEV/ST⁻HVD/GFP variant demonstrated similarly efficient replication in another cell line of vertebrate origin, NIH 3T3 cells (data not shown), but virus growth was strongly affected in mosquito C7/10 cells (Fig. 1D). Thus, the data suggested that VEEV can

1 µg of *in vitro*-synthesized RNA. One-fifth of the electroporated cells were seeded into 35-mm dishes, and media were replaced at the indicated time points. Virus titers were measured by a plaque assay on BHK-21 cells. (D) Replication of the designed VEEV/ST⁻HVD/GFP and control VEEV/GFP viruses in mosquito C7/10 cells. Cells were infected by the indicated viruses at an MOI of 5 PFU/cell. Media were harvested at the indicated time points, and titers were measured by a plaque assay on BHK-21 cells. The experiments were repeated 2 times, with very similar results.
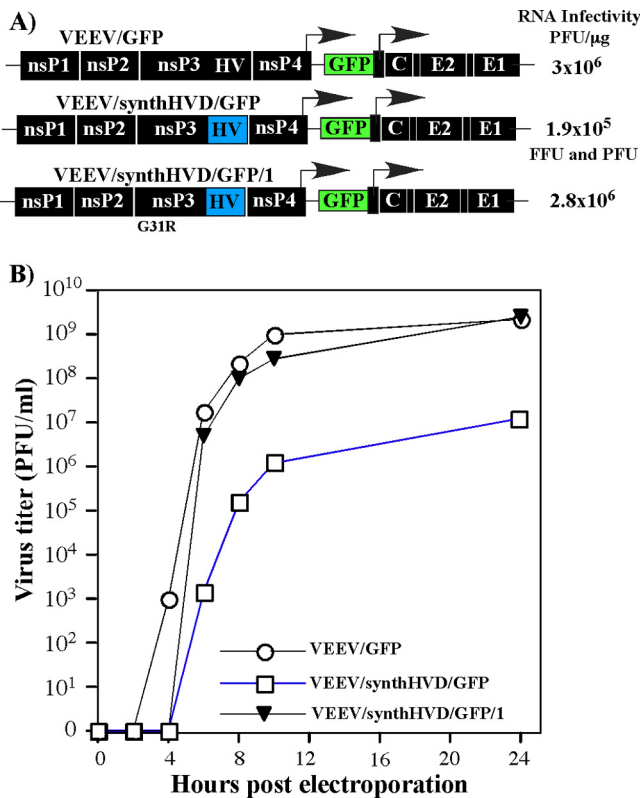
FIG 2 Extensive mutagenesis of the ST⁻ HVD has a negative effect on VEEV replication. (A) Schematic representation of VEEV/GFP, VEEV/synthHVD/GFP, and VEEV/synthHVD/GFP/1 virus genomes and infectivities of the *in vitro*-synthesized RNAs in the infectious center assay. VEEV/synthHVD/GFP/1 contained a G31R adaptive mutation in nsP3 (see Results for details). (B) One microgram of each *in vitro*-synthesized RNA was electroporated into BHK-21 cells. One-fifth of each sample was seeded into 35-mm dishes, and media were replaced at the indicated time points. Virus titers were measured by a plaque assay on BHK-21 cells. This experiment was repeated three times, with very similar results.
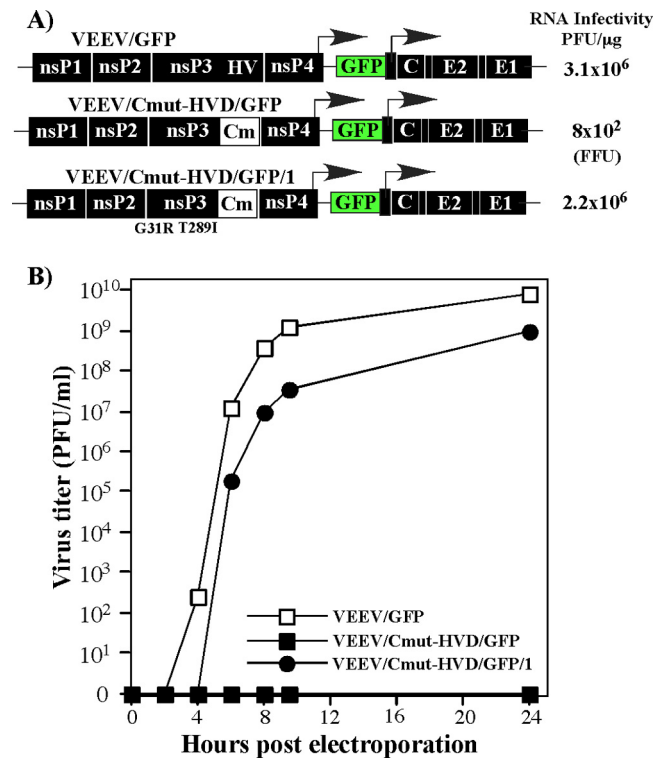
FIG 3 Replacement of the VEEV HVD with the amino terminus of mutated VEEV capsid protein has a negative effect on VEEV replication. (A) Schematic representation of VEEV/GFP, VEEV/Cmut-HVD/GFP, and VEEV/Cmut-HVD/GFP/1 virus genomes and infectivities of the *in vitro*-synthesized RNAs in the infectious center assay. A description of the amino-terminal fragment of VEEV capsid is presented in Results, and the sequence was reported previously [47]. VEEV/Cmut-HVD/GFP/1 contained additional adaptive mutations in nsP3, which strongly increased virus replication. (B) One microgram of each *in vitro*-synthesized RNA was electroporated into BHK-21 cells. One-fifth of each sample was seeded into 35-mm dishes, and media were replaced at the indicated time points. Virus titers were measured by a plaque assay on BHK-21 cells. This experiment was repeated three times, with very similar results.

tolerate extensive mutagenesis in the HVD without a strong negative effect on virus titers in vertebrate cells. The overall effect of these 53 mutations is detectable but would probably be difficult to study and interpret because of the small difference in replication rates between the original and mutant viruses. However, the removal of the potential phosphorylation sites, represented by Ser and Thr, from the HVD has a more marked effect on VEEV replication in a mosquito cell line.

VEEV can tolerate strong modifications to the HVD and evolves to more efficient replication. The experiments described above demonstrated that 53 point mutations in the VEEV HVD had no profound effect on VEEV replication in vertebrate cells, suggesting that the amino acid sequence of the HVD does not play a significant role in the fragment's function. However, the following experiments demonstrated that this was not the case. Our next step was to introduce additional mutations into the nsP3 HVD of the VEEV/ST⁻HVD/GFP variant by changing the positions of all of the encoded amino acids in this already modified nsP3 domain. Thus, neither the codon usage in the gene nor the amino acid composition of the HVD was additionally changed. The mutations also did not change the overall hydrophobicity profile of the HVD, and based on computer modeling, this domain did not

attain a stable secondary structure (data not shown). However, this scrambled version of the HVD produced a profound negative effect on virus replication. In the infectious center assay, the *in vitro*-synthesized RNA of the designed VEEV/synthHVD/GFP variant generated a mixture of GFP-positive cell foci and plaques, and the overall efficiency of their formation was almost 20-fold lower than that of the control VEEV/GFP RNA (Fig. 2A). In multiple repeated experiments, after electroporation of the *in vitro*-synthesized RNA into BHK-21 cells, VEEV/synthHVD/GFP demonstrated lower replication rates, with titers not exceeding 10^7 PFU and FFU per ml (Fig. 2B). Thus, extensive mutagenesis of the VEEV HVD sequence strongly affected virus replication. However, VEEV/synthHVD/GFP rapidly evolved to a more efficiently replicating, plaque-forming phenotype. Based on our previous experience, we surmised that the 20-fold difference in RNA infectivity indicated that the initially designed variant was capable of inefficient replication in this cell line and that evolution leading to more efficient infection spread and plaque formation was likely the result of a very limited number of adaptive mutations (most likely a single mutation) in the viral genome. The development of both plaques and foci in the infectious center assay was also sug-
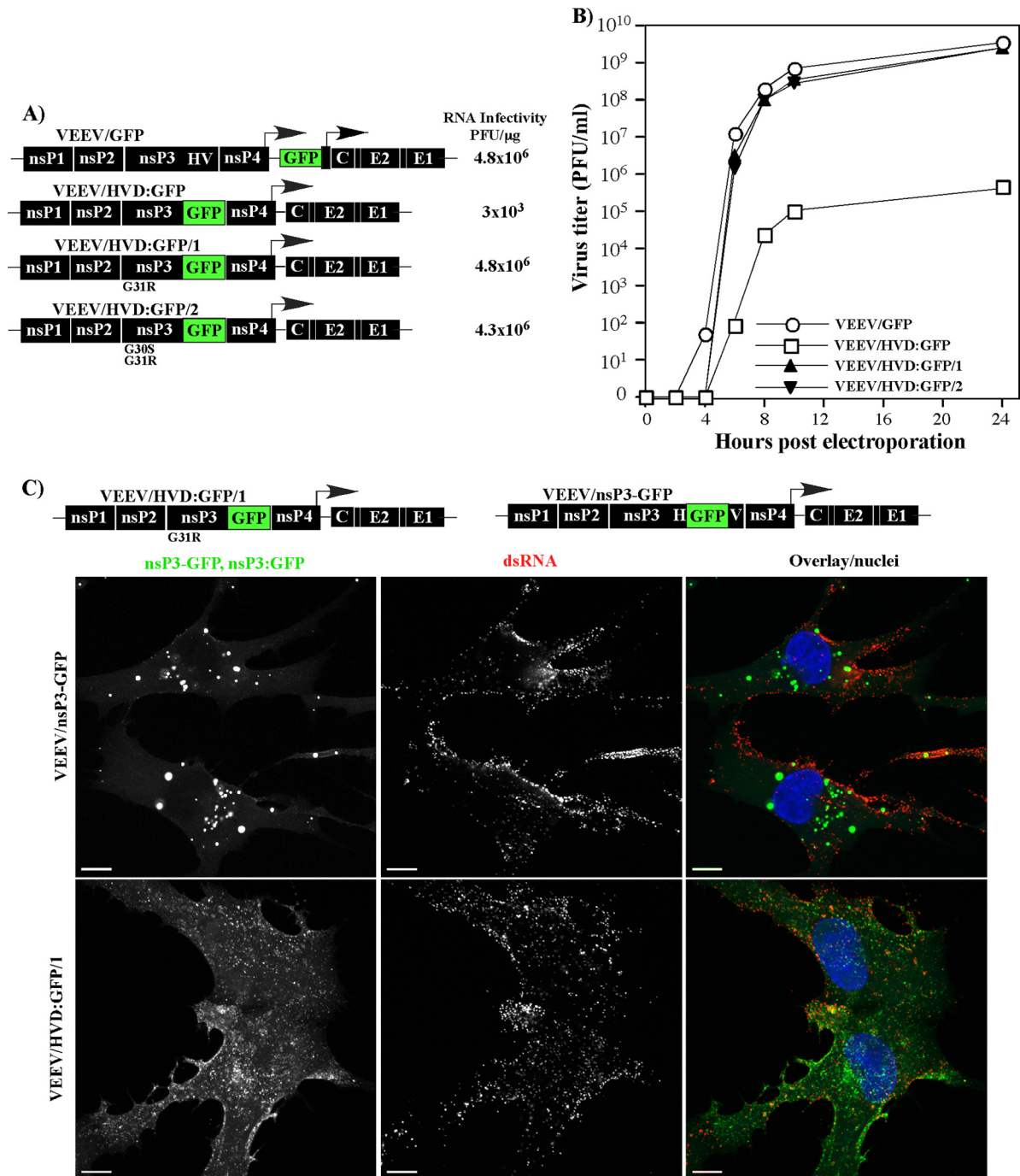
FIG 4 Replacement of the VEEV HVD with GFP strongly affects virus replication in BHK-21 cells. (A) Schematic representation of VEEV/GFP, VEEV/HVD:GFP, VEEV/HVD:GFP/1, and VEEV/HVD:GFP/2 virus genomes and infectivities of the *in vitro*-synthesized RNAs in the infectious center assay. VEEV/HVD:GFP/1 and VEEV/HVD:GFP/1 contained additional adaptive mutations in nsP3. These mutations strongly increased virus replication. (B) One microgram of each *in vitro*-synthesized RNA was electroporated into BHK-21 cells. One-fifth of each sample was seeded into 35-mm dishes, and media were replaced at the indicated time points. Virus titers were measured by a plaque assay on BHK-21 cells. This experiment was repeated twice, with very similar results. (C) Compartmentalization of (i) VEEV nsP3, containing a GFP replacement of the HVD and an adaptive mutation in the amino-terminal domain, and (ii) virus-specific dsRNA in BHK-21 cells. BHK-21 cells in Ibidi 8-well μ-slides were infected with the indicated viruses at an MOI of 20 infectious units/cell. At 6 h postinfection, cells were fixed, permeabilized, and stained with a dsRNA-specific MAb, an Alexa Fluor 555-labeled secondary antibody, and Hoechst dye (nuclei). Images are presented as multiple-intensity projections of six optical sections in the middle plane of the nuclei. Bars correspond to 10 μm. The VEEV/nsP3-GFP variant was used to demonstrate the natural distribution of nsP3 and dsRNA in VEEV-infected cells. This mutant contained a GFP insertion into the wt HVD and was described previously (41). The insertion has been shown to have no effect on VEEV replication and formation of protein complexes.

gestive that the acquired adaptive mutations had different effects on virus replication.

In another mutant, we replaced the entire HVD-encoding sequence, with the exception of the last 5 aa, with either a fragment encoding the 97-aa-long amino-terminal domain of the wild-type (wt) VEEV capsid protein or the same-length fragment representing a mutated version of the amino-terminal capsid's domain, which we developed in our previous studies (Fig. 3A) (47, 48). This choice was made based on the fact that the amino terminus of VEEV capsid, except for a very short predicted helix I, is not folded into a secondary structure. Replacement of the nsP3 HVD with the wt capsid sequence was lethal, and no viable virus was recovered after repeated electroporations of the *in vitro*-synthesized RNA (data not shown). However, the second, mutated, capsid-specific amino acid sequence had almost all of the positively charged amino acids replaced by Gly, Ala, Ser, and Asn. Thus, the latter sequence mimicked to some extent the natural VEEV nsP3 HVD, although it was 2-fold shorter. In the infectious center assay, the *in vitro*-synthesized RNA of VEEV/Cmut-HVD/GFP demonstrated very low infectivity. Very few cells demonstrated GFP expression and induced the formation of GFP-positive foci (Fig. 3A). However, as in the above-described experiments with VEEV/synthHVD/GFP, the new variant was capable of evolving to a more efficiently replicating phenotype, and after three passages on BHK-21 cells, we selected variants demonstrating efficient replication and plaque formation. This indicated that after acquiring a small number of adaptive mutations, the VEEV/Cmut-HVD/GFP variant was capable of replication in BHK-21 cells.

In complementing experiments, another substantial change was introduced into VEEV nsP3 by replacing its HVD with that encoding the completely unrelated GFP (VEEV/HVD:GFP). The only remnants of the wt HVD amino acid sequence were the 5 carboxy-terminal amino acids, which were retained to allow proper function of the stop codon, located between nsP3- and nsP4-encoding sequences, and a few amino acids upstream of the P34 cleavage site. In contrast to the above-described replacement fragments, which were unfolded, GFP has a well-defined globular structure, and no GFP interaction with any cellular proteins has previously been described. This major replacement initially had a strong negative effect on the infectivity of the *in vitro*-synthesized RNA (Fig. 4A), but as in the cases of VEEV/synthHVD/GFP and VEEV/Cmut-HVD/GFP, efficiently replicating variants of VEEV/HVD:GFP were selected within a few passages. In BHK-21 cells, they demonstrated a plaque-forming, cytopathic phenotype. Thus, VEEV nsP3 was able to support virus replication even when its natural unstructured HVD was replaced by the highly structured GFP. However, adaptive mutations were also required.

To further analyze the adaptive mutations, we passaged VEEV/synthHVD/GFP, VEEV/Cmut-HVD/GFP, and VEEV/HVD:GFP virus populations using gradually decreasing volumes of media harvested after each previous passage. This passaging was aimed at enriching virus populations with the most efficiently replicating variants. The adapted variants were then isolated from 2 or 3 randomly selected plaques, and their nsP3 and nsP2 genes were sequenced to identify adaptive mutations. Sequencing produced strikingly consistent results. The evolved, efficiently replicating variants of all three constructs contained mutations in the same position, Gly31 of nsP3 (G31R mutation). Only one of the plaque isolates of VEEV/HVD:GFP contained a double mutation in nsP3 (G30S and G31R). The isolates of VEEV/Cmut-HVD/GFP con-
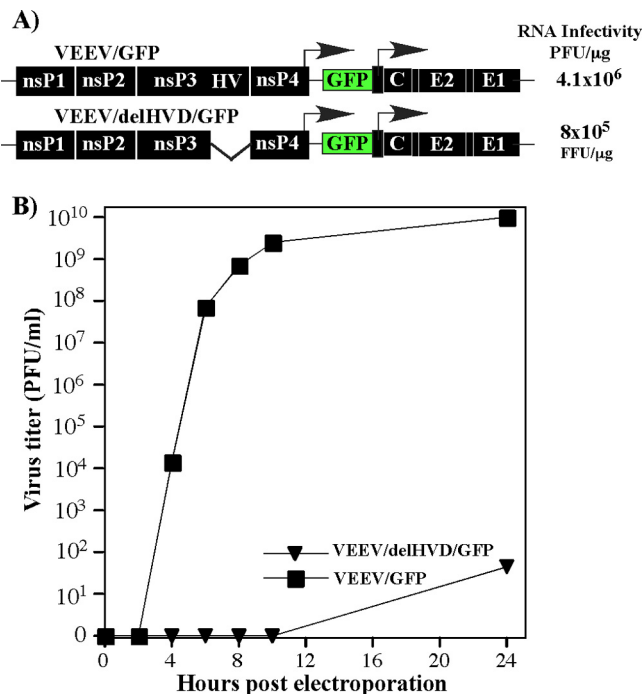

FIG 5 Deletion of the entire VEEV HVD has a deleterious effect on VEEV replication in BHK-21 cells. (A) Schematic representation of the VEEV/GFP and VEEV/delHVD/GFP genomes and infectivities of the *in vitro*-synthesized RNAs in the infectious center assay. A description of the deletion is presented in Results. (B) One microgram of each *in vitro*-synthesized RNA was electroporated into BHK-21 cells. One-fifth of each sample was seeded into 35-mm dishes, and media were replaced at the indicated time points. Virus titers were measured by a plaque assay on BHK-21 cells. This experiment was repeated twice, with very similar results.

tained, in addition to G31R, a T289I mutation in nsP3. This double mutation correlated with a relatively low efficiency of appearance of adapted, plaque-forming variants (Fig. 3A). Therefore, in the following experiments, both of these mutations were cloned into the originally designed construct.

To confirm the stimulatory effects of the mutations on virus replication, all of them were cloned into the original, corresponding cDNAs to generate (i) VEEV/synthHVD/GFP/1, having G31R mutations (Fig. 2A); (ii) VEEV/Cmut-HVD/GFP/1, containing G31R and T289I mutations (Fig. 3A); and (iii) VEEV/HVD:GFP/1 and VEEV/HVD:GFP/2, containing a G31R mutation and both G31R and G30S mutations, respectively (Fig. 4A). The introduced mutations resulted in RNA infectivities and virus replication rates in BHK-21 cells that were very similar to those of the control viruses encoding wt nsP3 (Fig. 2B, 3B, and 4B). In spite of containing an essentially scrambled amino acid sequence in the HVD (VEEV/synthHVD/GFP/1) or having this fragment replaced with GFP (VEEV/HVD:GFP/1) or a mutated capsid protein-encoding sequence (VEEV/Cmut-HVD/GFP/1), the adapted variants were capable of developing productive, spreading infection in BHK-21 cells. The second G30S mutation in VEEV/HVD:GFP/2 did not demonstrate a noticeable, additional stimulatory effect on replication. The distinguishing feature of VEEV/HVD:GFP/1 was its inability to form the previously described, large, nsP3-containing complexes, which are normally present in cells infected with VEEV (Fig. 4C). Most of this fusion protein, which lacked the
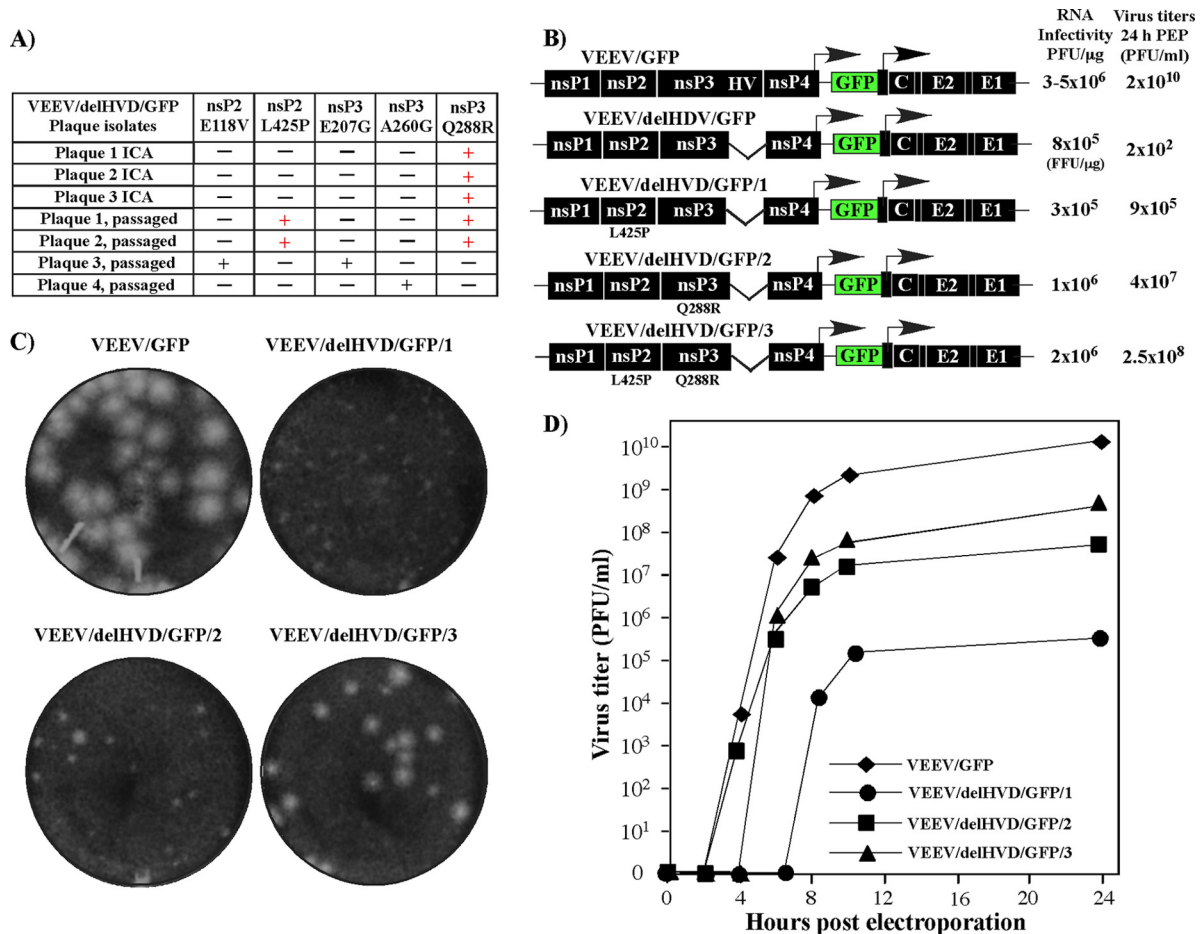
A)

VEEV/delHVD/GFP Plaque isolates	nsP2 E118V	nsP2 L425P	nsP3 E207G	nsP3 A260G	nsP3 Q288R
Plaque 1 ICA	−	−	−	−	+
Plaque 2 ICA	−	−	−	−	+
Plaque 3 ICA	−	−	−	−	+
Plaque 1, passaged	−	+	−	−	+
Plaque 2, passaged	−	+	−	−	+
Plaque 3, passaged	+	−	+	−	−
Plaque 4, passaged	−	−	−	+	−

B)

C)

D)

FIG 6 The VEEV/delHVD/GFP variant rapidly develops adaptive mutations in nsP2 and nsP3, which increase virus replication in BHK-21 cells. (A) List of putative adaptive mutations identified in VEEV/delHVD/GFP variants, which were plaque purified either directly after RNA electroporation in the infectious center assay (ICA) or after a few rounds of passaging in BHK-21 cells. (B) Schematic representation of VEEV/GFP, VEEV/delHVD/GFP, and VEEV/delHVD/GFP variants containing the most common mutations in their nsPs. RNA infectivities in the infectious center assay and virus titers at 24 h postelectroporation (PEP) of 1 μg of the *in vitro*-synthesized RNAs into BHK-21 cells are indicated. (C) Plaques developed by the indicated variants in the infectious center assay. Plaques were stained by crystal violet at 48 h post-RNA electroporation. (D) Replication rates of the indicated virus variants after electroporation of 1 μg of the *in vitro*-synthesized RNAs into BHK-21 cells. One-fifth of each sample was seeded into 35-mm dishes, and media were replaced at the indicated time points. Virus titers were measured by a plaque assay on BHK-21 cells. This experiment was repeated twice, with very similar results.

natural HVD, was diffusely distributed in the infected cells (Fig. 4C). It formed more dense structures in close proximity to the viral replication complexes, which were stained with dsRNA-specific MAb. This distribution of the nsP3:GFP fusion was similar to that of wt nsP3 at early times postinfection (p.i.) (2 h) with wt VEEV (41).

Taken together, the data suggested that the VEEV HVD does not play a critical role in VEEV replication in BHK-21 cells. It can be replaced by heterologous polypeptides, and replication of such variants requires only one or two adaptive mutations in the conserved, amino-terminal nsP3 domain to become comparable to replication of VEEV encoding wt nsP3.

Deletions in the VEEV HVD differentially affect virus replication. The data presented above suggested that the VEEV HVD is dispensable for virus replication. However, the results of previously reported studies demonstrated that extensive deletions of the nsP3 HVD of SFV made this virus nonviable (49). This discrepancy could be explained by the abundant differences between the Old World and New World alphavirus groups. Another pos-

sibility is that a lack of plaque-forming activity is not necessarily an indication that viruses are not viable. They may exhibit a reduced replication efficiency and become incapable of causing CPE but go on to demonstrate further evolution, which is not easy to detect. Therefore, to further understand the function of the HVD in the context of VEEV, we performed an additional set of experiments with the VEEV HVD deletion mutant.

We produced a cDNA for the VEEV/delHVD/GFP variant, which lacked the entire HVD except for the last 5 aa located upstream of the termination codon. To detect viral RNA replication and monitor the spread of infection, a GFP marker was cloned into the viral genome under the control of a subgenomic promoter, as in the above-described mutants (Fig. 5A). The infectious center assay on BHK-21 cells demonstrated that the designed deletion mutant was capable of producing small foci of GFP-positive cells with almost the same efficiency as VEEV/GFP (Fig. 5A). Within 24 h post-RNA transfection, it also became capable of producing cytopathic infectious virus, and samples harvested at 24 h postelectroporation already contained plaque-forming variants
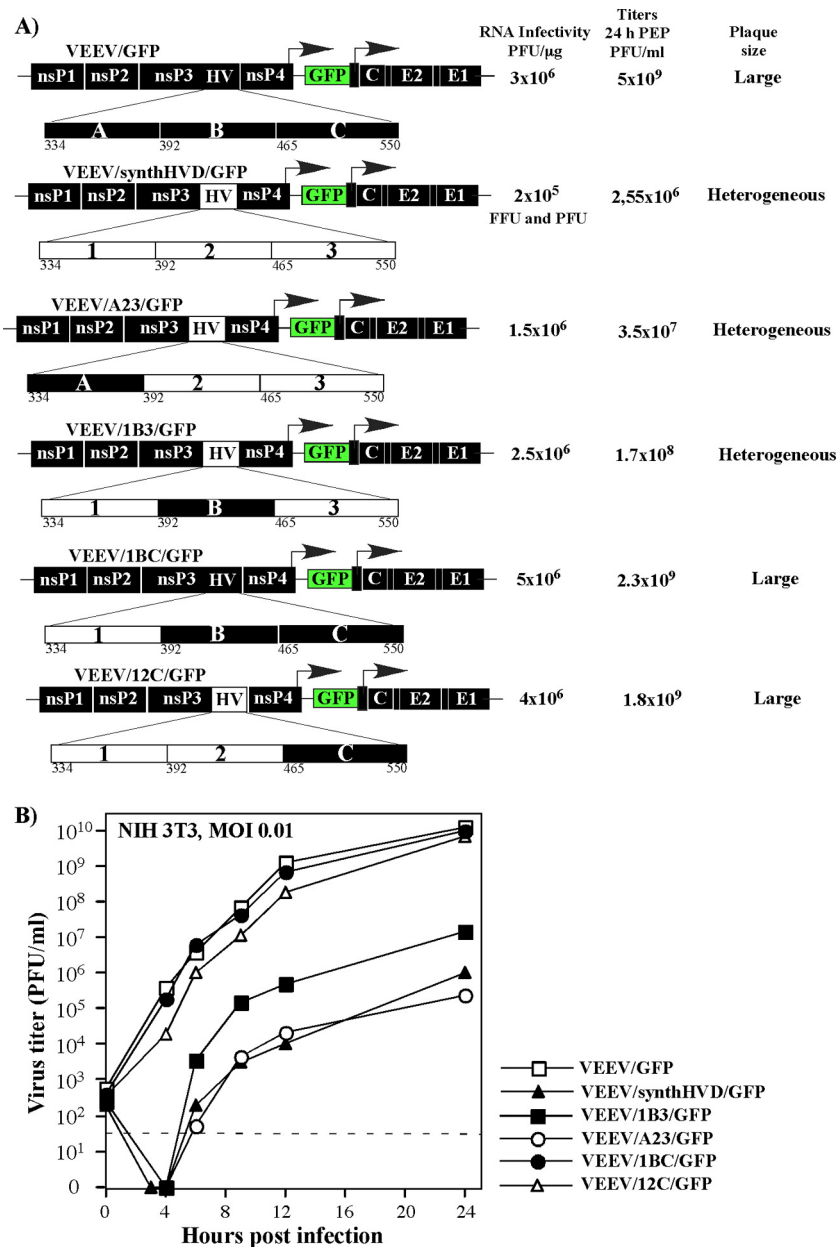
FIG 7 The carboxy-terminal fragment of the VEEV nsP3-specific HVD plays a critical role in VEEV replication in BHK-21 and NIH 3T3 cells. (A) Schematic representation of VEEV genomes containing the nsP3 HVD assembled from different fragments of the wt HVD and those derived from VEEV/synthHVD/GFP. RNA infectivities in the infectious center assay, virus titers at 24 h postelectroporation, and plaque morphology of virus stocks are indicated. (B) Replication rates of the indicated VEEV variants in NIH 3T3 cells. A total of 5×10^5 NIH 3T3 cells in 6-well Costar plates were infected with the indicated viruses at an MOI of 0.01 PFU/cell. At the indicated time points, media were replaced, and virus titers were determined by a plaque assay on BHK-21 cells. This experiment was repeated twice, with very similar results.

(Fig. 5B). Thus, the deletion had a negative effect on virus replication, but the deletion mutant likely accumulated adaptive mutations, which compensated for the deletion's negative effect.

In these experiments, we randomly selected both a few plaques after titration of the serially passaged stocks and a few of those formed in the infectious center assay. In all of the plaque-isolated variants, both the nsP2 and nsP3 genes were sequenced, and the identified mutations are presented in Fig. 6A. In contrast to the pseudorevertants of VEEV/synthHVD/GFP, VEEV/Cmut-HVD/GFP, and VEEV/HVD:GFP in the earlier experiments, mutations

were identified not only in nsP3 but also in nsP2. We cloned the most representative mutations (L425P in nsP2 and Q288R in nsP3) and a combination of both into the originally designed VEEV/delHVD/GFP cDNAs and tested their effects on virus replication. The adaptive mutations made viruses capable of forming plaques, which were readily visible in the infectious center assay (Fig. 6B); they also increased virus replication rates and final titers (Fig. 6C and D). The VEEV/delHVD/GFP/1 variant containing the adaptive mutation in nsP2 formed pinpoint plaques, produced low-titer stocks, and was unstable, capable of further evo-

lution. The nsP3-specific mutation in VEEV/delHVD/GFP/2 produced a greater increase in virus titers but similarly did not increase the cytopathogenicity. It formed only very small plaques. However, a combination of both mutations in VEEV/delHVD/GFP/3 strongly improved the ability of the virus to cause a cytopathic effect and increased the plaque size. This was an indication that the mutations functioned synergistically in the development of a spreading and cytopathic virus phenotype.

Thus, VEEV could tolerate the deletion of the entire HVD. Such an extended deletion had deleterious effects on virus replication in BHK-21 cells and made it noncytopathic. However, the deletion is not lethal and can be compensated for by adaptive mutations in the viral nonstructural genes.

The repeating element in the VEEV HVD determines virus replication in a cell-specific mode. The experiments described above suggested that the HVD deletion and its replacement with heterologous protein-encoding sequences could be compensated for by point mutations, appearing mostly in the conserved domain of the nsP3 protein. These adapted mutants were capable of replication and CPE development. However, this efficiently replicating phenotype was specific exclusively for BHK-21 cells. None of these pseudorevertants was able to develop efficient replication and spreading infection in any other cells of either mosquito or vertebrate origin, such as Vero cells, NIH 3T3 cells, IFN-α/βR$^{-/-}$ mouse embryonic fibroblasts (MEFs), HeLa cells, and HEK293 cells. Moreover, in spite of numerous attempts, these pseudorevertants demonstrated no adaptation to replication in these cell lines to high titers (data not shown). These experiments indicated that the HVD does function in virus replication and that it functions in a cell-specific mode.

The availability of mutants such as (i) VEEV/synthHVD/GFP, which is incapable of efficient, productive replication in vertebrate cells, with the exception of BHK-21 cells, and (ii) wt VEEV/GFP, which replicates efficiently in any tested cell type, suggested a means for the identification of a particular nsP3 HVD fragment, which plays a critical role in VEEV replication. Therefore, in the next experiments, we designed a set of recombinant viruses which contained combinations of fragments derived from VEEV/synth-HVD/GFP and VEEV/GFP in their HVDs (Fig. 7A). These recombinant viral genomes were tested by the infectious center assay for final titers at 24 h postelectroporation and for replication rates in NIH 3T3 cells. Some of these mutants demonstrated inefficient replication in BHK-21 cells, with subsequent rapid evolution to a more cytopathic phenotype. However, the inability of nsP3 HVD mutants to efficiently replicate in NIH 3T3 cells (regardless of the presence of BHK-21-specific mutations) afforded us the opportunity to accurately assess the effects of the various fragment combinations on VEEV replication and establish the relative importance of each region of the HVD for VEEV replication in this cell line. Thus, we tested replication of the electroporation-derived viruses in NIH 3T3 cells in spite of the heterogeneity of virus populations used for infection (Fig. 7B). The replacement of the amino-terminal fragment 1 from VEEV/synthHVD/GFP with the corresponding sequence A, derived from the wt HVD (VEEV/A23/GFP variant), had no positive effect on virus replication. In NIH 3T3 cells, it was indistinguishable from VEEV/synthHVD/GFP. The replacement of the carboxy-terminal fragment 3 of VEEV/synthHVD/GFP with fragment C from the wt HVD (VEEV/12C/GFP) strongly increased virus titers in BHK-21 cells (Fig. 7A) and also made it capable of developing homogeneous
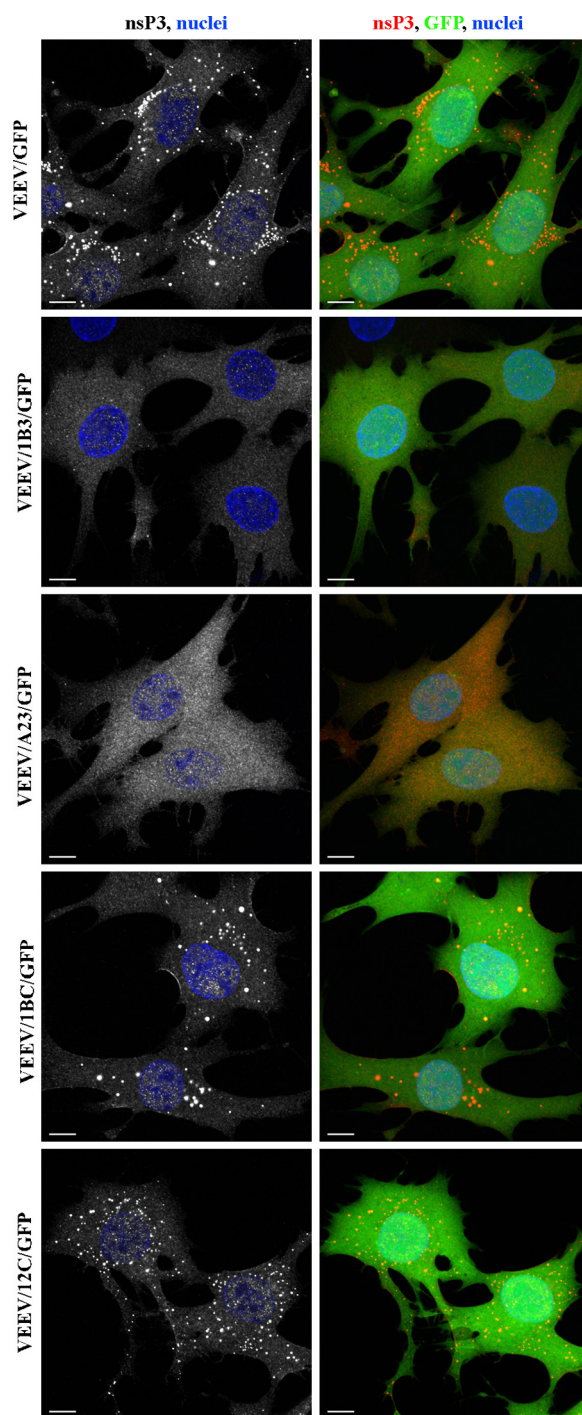

FIG 8 The carboxy-terminal fragment of the VEEV nsP3 HVD plays a critical role in protein complex formation. BHK-21 cells in Ibidi 8-well μ-slides were infected with the indicated viruses at an MOI of 20 infectious units/cell. At 6 h postinfection, cells were fixed, permeabilized, and stained with a VEEV nsP3-specific MAb, an Alexa Fluor 555-labeled secondary antibody, and Hoechst dye (nuclei). Images are presented as multiple-intensity projections of 6 optical sections. Bars correspond to 10 μm.

plaques and replicating in NIH 3T3 cells with almost the same efficiency as that of VEEV/GFP. The replacement of the middle fragment 2 in VEEV/synthHVD/GFP with fragment B from the wt HVD (VEEV/1B3/GFP) also demonstrated a detectable positive
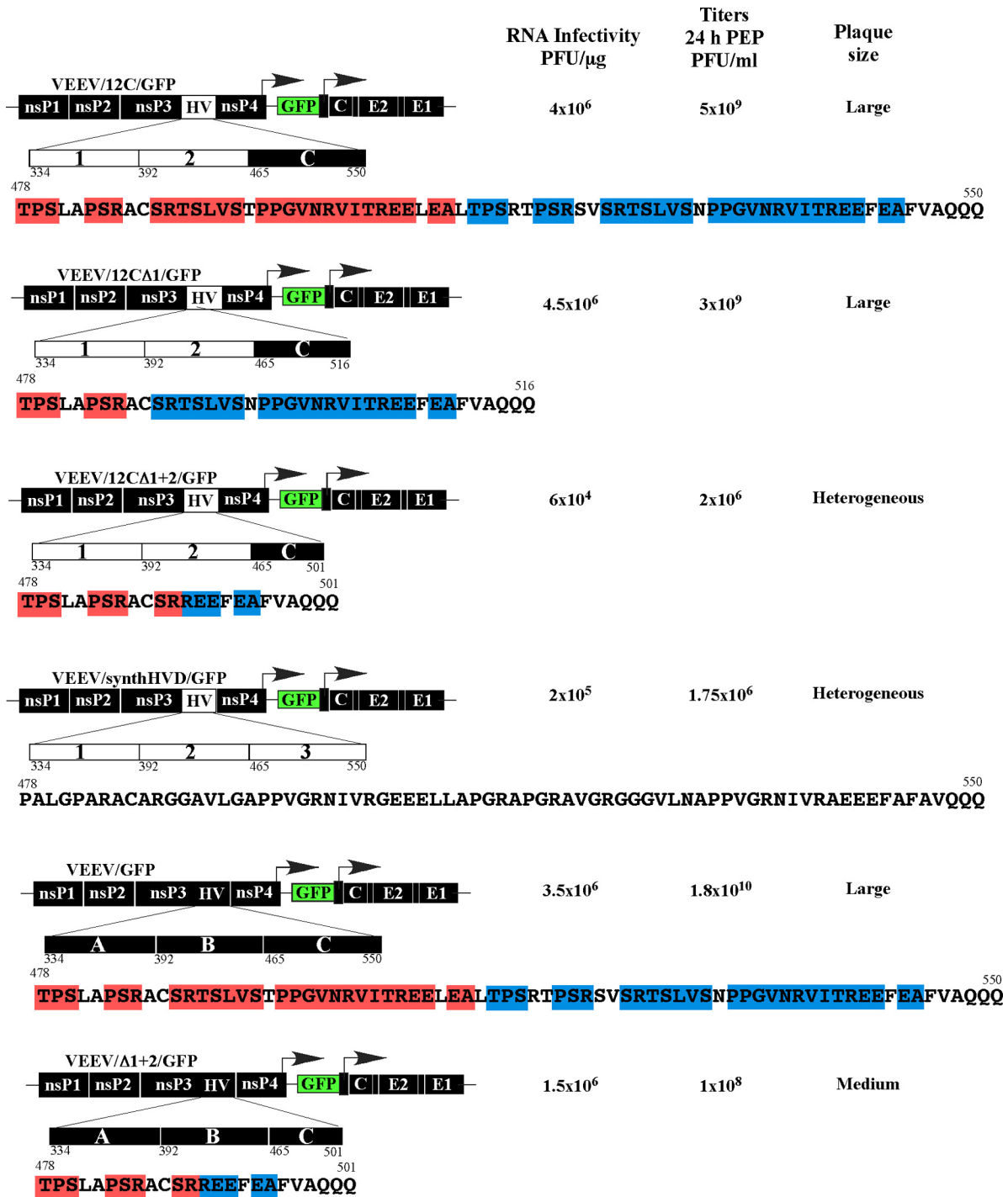
FIG 9 The carboxy-terminal duplicated element in the VEEV nsP3 HVD strongly determines the efficiency of VEEV replication in BHK-21 cells. Shown is a schematic representation of VEEV/12C/GFP and VEEV/GFP genomes with introduced mutations in the repeated elements, located at the carboxy terminus of the HVD (fragment C). Repeat 1 is indicated in red, and repeat 2 is indicated in blue. RNA infectivities in the infectious center assay, virus titers at 24 h postelectroporation, and plaque morphology of variants, which are present in virus stocks, are indicated.

effect on final virus titers in BHK-21 cells and its replication efficiency in NIH 3T3 cells (Fig. 7B). Fragment B also made replication of VEEV/1BC/GFP detectably more efficient than replication of VEEV/12C/GFP (Fig. 7B). However, the effect of the replacement of this middle fragment was dramatically smaller than that

of the carboxy-terminal fragment C. Thus, the data suggested that the carboxy-terminal HVD fragment (aa 465 to 550) is a critical determinant of VEEV replication in BHK-21 and NIH 3T3 cells in particular.

We previously described that in any infected cells, wt VEEV
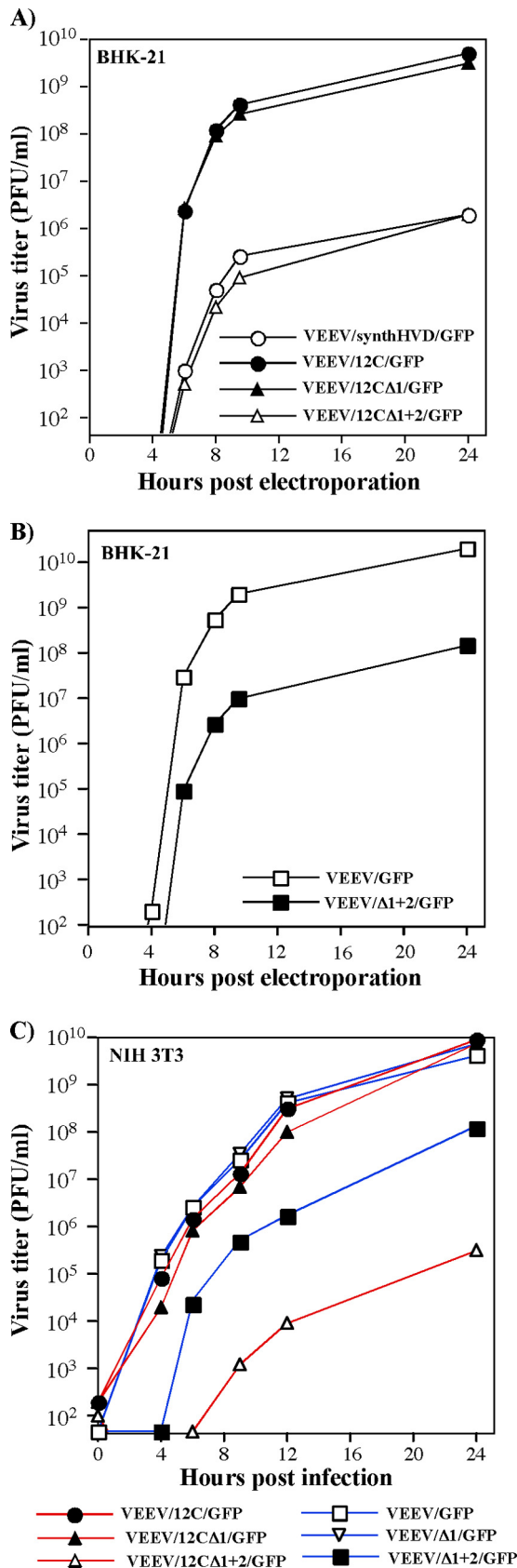
nsP3 forms large spherical structures (spheroids), and their pattern is determined by the HVD (41). Therefore, the designed mutants were also analyzed in terms of nsP3-specific complex formation in infected cells. BHK-21 cells were infected with the newly designed mutants and stained with MAb specific to the amino-terminal nsP3 domain (41). nsP3 with synthetic HVD (VEEV/synthHVD/GFP-infected cells) demonstrated a diffuse distribution (Fig. 8). Replacement of synthetic fragment 1 or 2 with the corresponding wt fragment A or B, respectively, did not change the diffuse intracellular distribution of the nsP3 mutant (VEEV/A23/GFP- and VEEV/1B3/GFP-infected cells) (Fig. 8). However, the replacement of fragment 3 with the corresponding fragment C (VEEV/12C/GFP) restored the ability of nsP3 to form spheroid-like structures albeit of a noticeably smaller size. VEEV/1BC/GFP, which had wt B and C fragments, was indistinguishable from VEEV/GFP in terms of nsP3-specific complex formation. Thus, the C fragment was found to be a critical determinant of nsP3 protein complex formation.

The distinguishing feature of this carboxy-terminal fragment C was the presence of 2 repeats of a 33-aa-long sequence (Fig. 9). In the next round of experiments, we deleted either one of the repeated elements or both of them in the efficiently replicating VEEV/12C/GFP construct. The deletion of one of the repeats had no noticeable effect on virus replication in either the BHK-21 or NIH 3T3 cell line (Fig. 9 and 10). VEEV/12CΔ1/GFP was capable of developing large homogeneous plaques, and its growth rates were indistinguishable from those of the parental VEEV/12C/GFP construct. However, an additional deletion of only 15 aa, which destroyed the second element, had a marked deleterious effect on virus replication. Titers and growth rates of VEEV/12CΔ1+2/GFP became 4 orders of magnitude lower than those of the parental VEE/12C/GFP construct. This indicated that the repeated sequence in the VEEV nsP3-specific HVD plays a critical role in virus replication.

The indicated repeats also played an important role in the replication of VEEV with the wt HVD. The replication rates of the VEEV/Δ1/GFP variant with one of the repeats deleted were indistinguishable from those of VEEV/GFP in both NIH 3T3 and BHK-21 cells (Fig. 10C and data not shown), but the titers of VEEV/Δ1+2/GFP, which no longer encoded both repeats, were at least 100-fold lower than those of VEEV/GFP at any time postinfection or post-RNA transfection (Fig. 10B and C).

Importantly, the deletion of both, but not the single, repeats in VEEV/12C/GFP made VEEV/12CΔ1+2/GFP incapable of form-

FIG 10 Deletion of one repeat element can be tolerated by the virus, but deletion of both repeats has deleterious effects on VEEV replication in both BHK-21 and NIH 3T3 cells. (A) Replication of VEEV/12C/GFP variants with deletions of one or both repeats in fragment C in BHK-21 cells. A detailed description of the deletions is presented in Fig. 9. (B) Replication of VEEV/GFP and VEEV/Δ1+2/GFP variants in BHK-21 cells. A detailed description of the deletion is presented in Fig. 9. For panels A and B, 1 μg of the in vitro-synthesized RNAs was electroporated into BHK-21 cells. One-fifth of each sample was seeded into 35-mm dishes, and media were replaced at the indicated time points. Virus titers were measured by a plaque assay on BHK-21 cells. VEEV/Δ1/GFP was not used in this experiment, because its efficient replication in this cell line was previously described (70). (C) Replication rates of the indicated virus variants in NIH 3T3 cells. A total of 5×10^5 NIH 3T3 cells in 6-well Costar plates were infected with the indicated viruses at an MOI of 0.01 PFU/cell. At the indicated time points, media were replaced, and virus titers were determined by a plaque assay on BHK-21 cells.
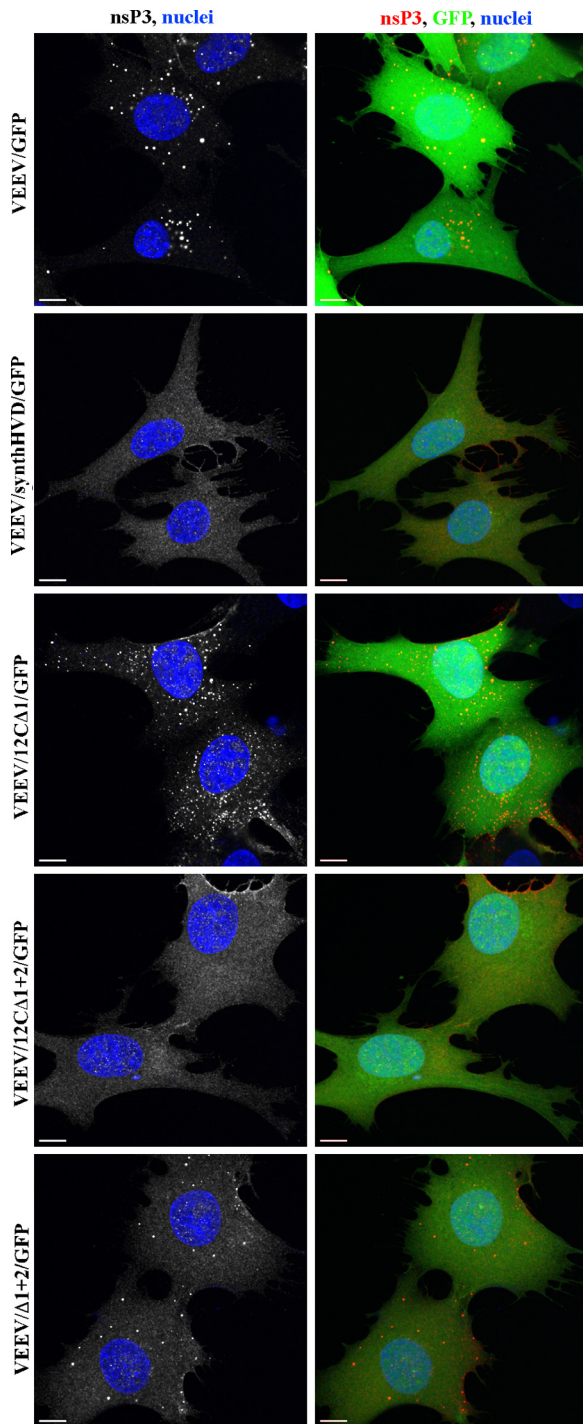
FIG 11 The carboxy-terminal repeat in the VEEV nsP3 HVD plays a critical role in protein complex formation. BHK-21 cells in Ibidi 8-well μ-slides were infected with the indicated viruses at an MOI of 20 infectious units/cell. At 6 h postinfection, cells were fixed, permeabilized, and stained with a VEEV nsP3-specific MAb, an Alexa Fluor 555-labeled secondary antibody, and Hoechst dye (nuclei). Images are presented as multiple-intensity projections of 6 optical sections. All images were acquired and processed with the same settings. Bars correspond to 10 μm.

ing large, nsP3-specific complexes (Fig. 11). Similar deletion of the repeats in the context of wt nsP3 (VEEV/Δ1+2/GFP) also had a very strong negative effect on the complex appearance, but very few and very small complexes could be found in essentially every infected cell. Their inefficient formation correlated with less efficient replication of the virus. However, the appearance of these small, but detectable, complexes and the higher replication rates of VEEV/Δ1+2/GFP than those of VEEV/12CΔ1+2/GFP also indicated that other HVD fragments (most likely fragment B) can to some extent compensate for the deletion of the repeats.

DISCUSSION

Within the last few years, great progress has been made in the understanding of the structure of alphavirus particles and the functions of both structural and nonstructural proteins in virus replication. Alphavirus nsP1, nsP2, and nsP4 were assigned multiple roles in viral RNA synthesis and modification of the intracellular environment (22, 23, 48, 50–62). However, one of the four nonstructural proteins, nsP3, remains insufficiently explored, and to date, its functions remain obscure. Similar to other viral nonstructural and structural proteins, nsP3 appears to be multifunctional and involved in a variety of processes which determine both RNA synthesis and intracellular-environment modification (10–12, 14, 29, 36, 41, 43, 63–66). This protein is an integral element of the alphavirus replication complexes, in which it interacts with other nsPs, and mutations in the nsP3-encoding sequence affect synthesis of the subgenomic RNA. The amino-terminal domain of nsP3, which is termed the macro domain (or X domain), is homologous to similar domains found in the proteins of other viruses with RNA-positive genomes in bacterial and some cellular proteins (33, 35). It has been experimentally demonstrated that nsP3 is capable of binding ADP-ribose, poly-ADP-ribose and short single-stranded RNA (ssRNA), although this has been shown to be a low-affinity interaction, and its biological significance is unclear (33). Mutations decreasing this interaction attenuate SINV, but this effect may have numerous explanations.

One of the most interesting structural features of alphavirus nsP3 is the presence of an approximately 200-aa-long, nonconserved HVD, whose function is far from being understood. In our recent studies, we demonstrated that VEEV and SINV HVDs tolerate large insertions, such as GFP- and Cherry-encoding sequences, without any noticeable effect on RNA and virus replication (12, 41). In VEEV and SINV, the HVDs were also interchangeable (41). The SINV- and VEEV-specific HVDs were equally efficient in VEEV replication. However, in the context of SINV, the VEEV-specific HVD functioned less efficiently in virus replication. This could be a result of interactions of virus-specific HVDs with different cellular proteins. In contrast to the SINV HVD, the VEEV-specific HVD demonstrated no binding to either G3BP1 or G3BP2, which is a hallmark of the Old World alphavirus interaction with vertebrate cells and is believed to facilitate competition with stress granule formation (10, 12, 14, 41, 63, 67). The VEEV nsP3 HVD also does not appear to possess the motifs that were recently proposed to interact with the Src homology 3 (SH3) domain of host cell amphiphysins Amph1 and Amph2. Their presence was shown to have a small but detectable stimulatory effect on RNA replication of the Old World alphaviruses (65).

The results of this study continue to demonstrate the unique characteristics of the VEEV nsP3-specific HVD. First, it is generally believed that the high concentration of serines and threonines
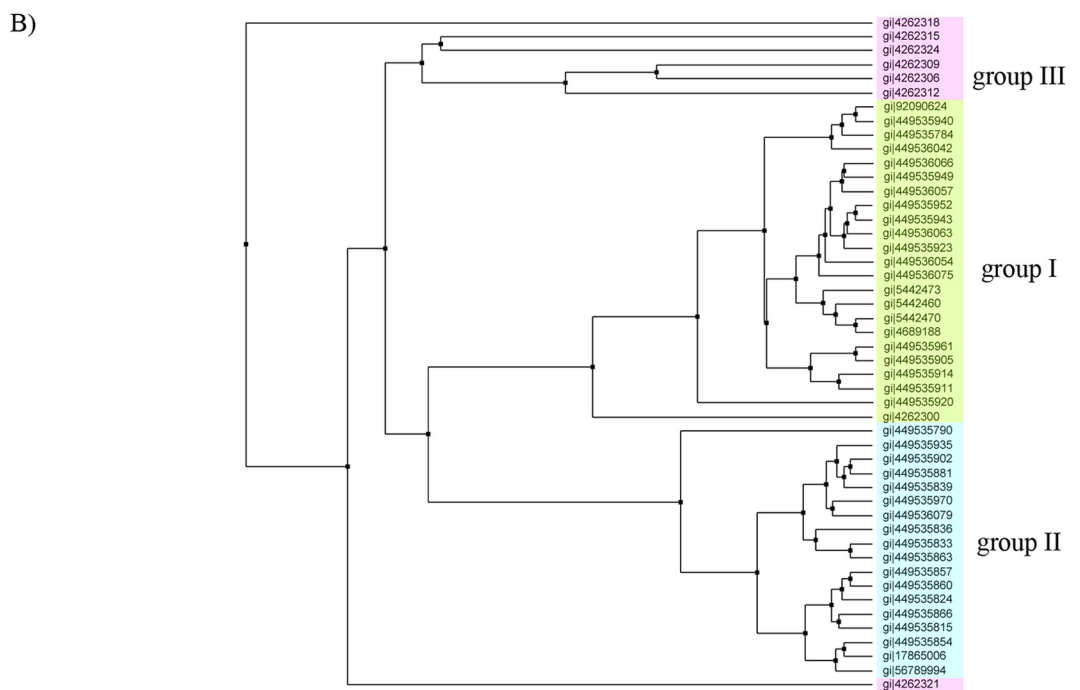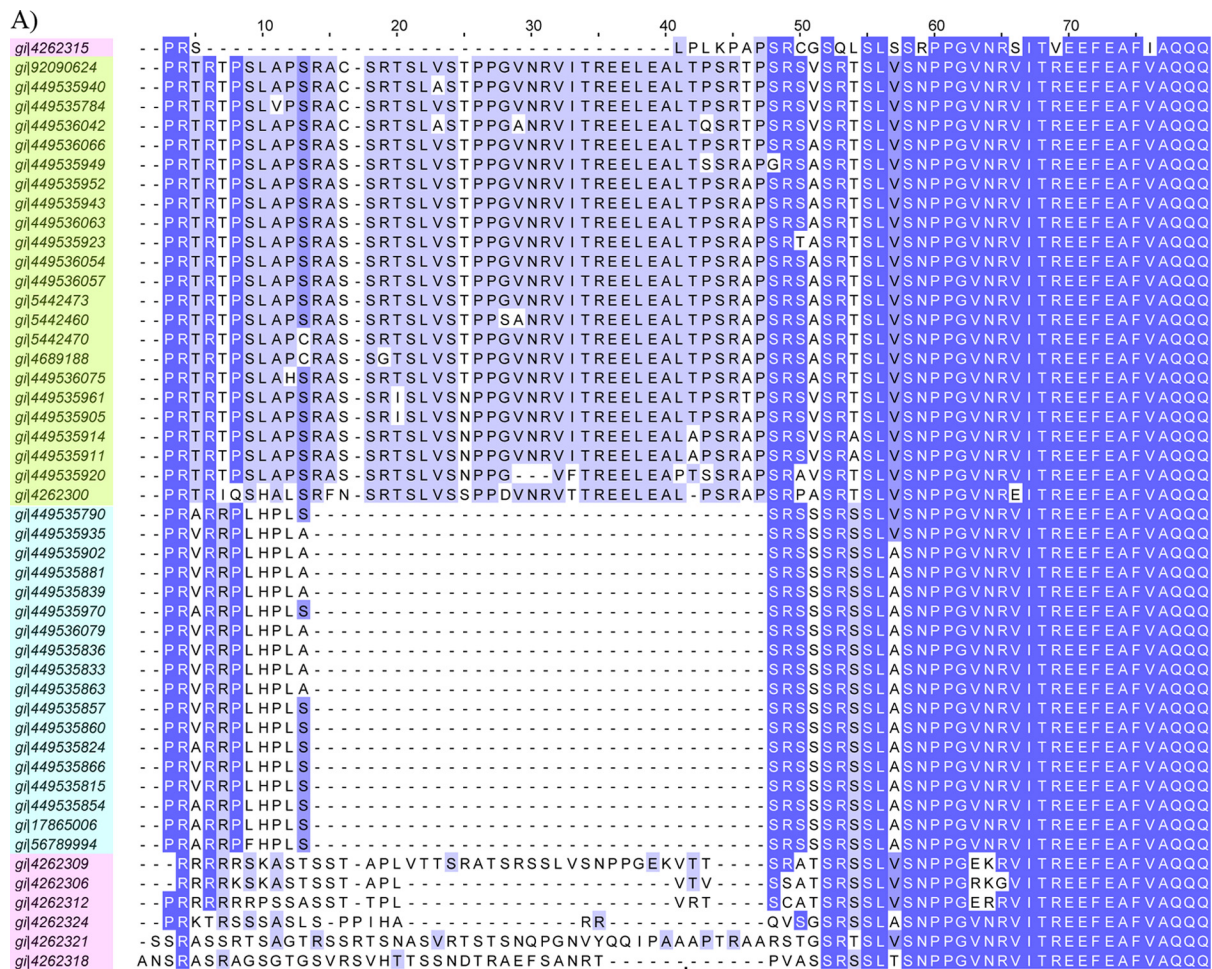
FIG 12 Members of the VEEV serocomplex demonstrate distinct evolution of the repeat located in the carboxy terminus of the nsP3 HVD. (A) Sequence alignment of the carboxy-terminal, repeat-containing fragments of the HVD of representative members of the VEEV serocomplex. All available sequences for VEEV nonstructural proteins were aligned by using ClustalW2. After removing all redundant sequences using a cutoff of 99%, the sequence corresponding to the carboxy-terminal repeated elements was copied and realigned by using the MATFF algorithm. Repeats are underlined using same colors as those used in Fig. 9. (B) The evolutionary tree of the VEEV serocomplex was built based on the amino acid sequences representing the entire nsP3 HVD.

in the HVDs of SINV and SFV is an indication of high phosphorylation levels of nsP3 and, thus, its importance for RNA and virus replication (42). However, in our experiments, the replacement of all of the serine- and threonine-specific codons, approximately 25% of the fragment, by those encoding other amino acids did not have a deleterious effect on VEEV replication. The detected small negative effect of the mutations on virus replication can be explained not only by a lack of phosphorylation but also by the overall strong change of the amino acid sequence.

Second, further disturbances to the VEEV nsP3 HVD sequence showed that, at least in the context of BHK-21 cells, the HVD can tolerate rearrangements, replacements, and deletions, requiring only one or two adaptive mutations in nsP3 or nsP2 to restore RNA infectivity and its replication to levels close to those of the wt. The strong colocalization of adaptive mutations in the codon for the conserved G31 was very surprising, since this amino acid was previously mutated in the context of wt SINV with only a small effect on replication (68). However, SINV and VEEV consistently demonstrate strong differences in their biology and virus-host interactions in particular. In other experiments performed in this study, we failed to select efficiently replicating SINV variants after making extensive deletions and replacements in the nsP3 HVD, which were similar to those described here for VEEV (data not shown). These results strongly support the notion that one needs to be very cautious when considering any alphavirus species to be models for others.

Third, the apparent plasticity of the VEEV HVD leading to an efficiently replicating phenotype was limited to the highly permissive BHK-21 cell line, and neither the originally designed VEEV nsP3 mutants nor the BHK-21-adapted variants could replicate efficiently in other tested cell lines. It remains unclear which particular characteristic(s) makes BHK-21 unique in terms of supporting replication of the mutant viruses. The most plausible explanation is that they are missing the negative protein regulator(s) of VEEV replication, whose activity is normally neutralized by the VEEV nsP3 HVD. The nature of this regulator is now under investigation. Based on our data, it is reasonable to expect that the critical element in this interaction might be the carboxy-terminal fragment of HVD. It contains an almost perfect repeat of 33 aa. The repeated elements demonstrate a redundant mode of function in virus replication. One of the repeats may be deleted without a noticeable effect on virus replication, but deletion of both of them has a profound negative effect on virus growth, particularly in cells other than BHK-21. Importantly, all of the members of the VEEV serocomplex demonstrate the presence of at least one of the elements of the repeat found in the nsP3 HVD, and based on the nsP3 HVD sequence alignment, naturally circulating VEEV strains can be divided into three major groups (Fig. 12): group I contains two repeats and groups II and III contain only one repeat at the nsP3 carboxy terminus. Interestingly, group I includes VEEV species (serotypes IAB, IC, and ID) known to be associated with high-level pathogenicity in humans and equids. It was previously demonstrated that the appearance of a duplicated amino acid sequence in Ross River virus nsP3 led to an increase of its pathogenicity in humans (69). In this study, the presence of two repeats supported noticeably higher VEEV replication rates; therefore, it is tempting to speculate that duplication of the described amino acid sequence in VEEV also led to the development of more pathogenic viruses. However, group II includes viruses belonging to serocomplex IE, which are also capable of developing

an epizootic phenotype. Importantly, this group contains an additional motif in the HVD that is not found in any other strains. Group III combined all other VEEV serotypes, which lack the above-described duplication and were never associated with human diseases. However, all of these serotypes are represented by single strains and have a high degree of heterogeneity in the HVD. Thus, all of the VEEV strains sequenced to date have at least one repeat in the HVD carboxy termini, and its duplication appears to correlate with increased pathogenicity in humans.

The critical role of the carboxy-terminal peptide in VEEV nsP3 function and the lack of such a peptide in the HVDs of other alphaviruses additionally demonstrate that each alphavirus appears to be unique in terms of virus-host interactions. In the case of VEEV, the repeated peptide is responsible for the formation of large, spherical, nsP3-containing protein complexes, which accumulate in the cytoplasm of infected cells (41). Their exact function remains unclear, since they are not sites of RNA replication and are very difficult to isolate. However, the defects in virus replication strongly correlate with the inability of nsP3 mutants to form these large complexes, despite the finding that, at least in BHK-21 cells, these mutants produce replication complexes and membrane spherules, which are locations of viral RNA synthesis (data not shown).

It appears to be unlikely that the carboxy-terminal repeat in the VEEV nsP3 HVD is the only functional sequence. First of all, alphaviruses and other RNA viruses do not encode nonessential genetic information. Second, the retention of the middle fragment B in the VEEV/1B3/GFP, VEEV/1BC/GFP, and VEEV/Δ1+2/GFP nsP3 mutants had a detectable positive effect on virus replication rates compared to those mutants lacking the B fragment. However, this effect was not as profound as that of the repeated sequences in the HVD carboxy terminus. This does not rule out the possibility that it might play a more important role in virus replication in the cells other than those used in this study.

Taken together, the results of this study demonstrate the following. (i) Phosphorylation of the VEEV nsP3-specific HVD is not a prerequisite for virus replication in cells of vertebrate, but not mosquito, origin. (ii) The VEEV HVD can be deleted or replaced by heterologous amino acid sequences, and these mutants rapidly attain the ability to replicate but only in BHK-21 cells. The latter cells are traditionally used for studying the mechanism of alphavirus replication, and thus, one needs to be more cautious in the interpretation of the BHK-21-derived data. (iii) The VEEV nsP3 HVD contains a carboxy-terminal repeated element, which plays a critical role in VEEV replication in cells other than BHK-21. This element plays a vital role in determining the formation of VEEV-specific protein complexes. Taken together, the results of this and previously reported studies suggest that the nsP3 HVD functions in a cell-specific mode and might play a critical role in virus adaptation to new cellular environments. This mode of action explains the high level of variability of the HVD between different alphaviruses, but this hypothesis needs further experimental support.

ACKNOWLEDGMENTS

REFERENCES

1. **Weaver SC, Barrett AD.** 2004. Transmission cycles, host range, evolution and emergence of arboviral disease. Nat. Rev. Microbiol. **2:**789–801.

2. **Weaver SC, Frolov I.** 2005. Togaviruses, p 1010–1024. *In* Mahy BWJ, ter Meulen V (ed), Virology, vol 2. Hodder Arnold, Salisbury, United Kingdom.

3. **Strauss JH, Strauss EG.** 1994. The alphaviruses: gene expression, replication, evolution. Microbiol. Rev. **58**:491–562.

4. **Griffin DE.** 1986. Alphavirus pathogenesis and immunity, p 209–250. *In* Schlesinger S, Schlesinger MJ (ed), The Togaviridae and Flaviviridae. Plenum Press, New York, NY.

5. **Angelini R, Finarelli AC, Angelini P, Po C, Petropulacos K, Macini P, Fiorentini C, Fortuna C, Venturi G, Romi R, Majori G, Nicoletti L, Rezza G, Cassone A.** 2007. An outbreak of chikungunya fever in the province of Ravenna, Italy. Euro Surveill. **12**(36):pii=3260. http://www.eurosurveillance.org/ViewArticle.aspx?ArticleId=3260.

6. **Angelini R, Finarelli AC, Angelini P, Po C, Petropulacos K, Silvi G, Macini P, Fortuna C, Venturi G, Magurano F, Fiorentini C, Marchi A, Benedetti E, Bucci P, Boros S, Romi R, Majori G, Ciufolini MG, Nicoletti L, Rezza G, Cassone A.** 2007. Chikungunya in north-eastern Italy: a summing up of the outbreak. Euro Surveill. **12**(47):pii=3313. http://www.eurosurveillance.org/ViewArticle.aspx?ArticleId=3313.

7. **Arankalle VA, Shrivastava S, Cherian S, Gunjikar RS, Walimbe AM, Jadhav SM, Sudeep AB, Mishra AC.** 2007. Genetic divergence of Chikungunya viruses in India (1963-2006) with special reference to the 2005-2006 explosive epidemic. J. Gen. Virol. **88**:1967–1976.

8. **Charrel RN, de Lamballerie X, Raoult D.** 2007. Chikungunya outbreaks—the globalization of vectorborne diseases. N. Engl. J. Med. **356**:769–771.

9. **Strauss EG, Rice CM, Strauss JH.** 1984. Complete nucleotide sequence of the genomic RNA of Sindbis virus. Virology **133**:92–110.

10. **Cristea IM, Carroll JW, Rout MP, Rice CM, Chait BT, MacDonald MR.** 2006. Tracking and elucidating alphavirus-host protein interactions. J. Biol. Chem. **281**:30269–30278.

11. **Cristea IM, Rozjabek H, Molloy KR, Karki S, White LL, Rice CM, Rout MP, Chait BT, MacDonald MR.** 2010. Host factors associated with the Sindbis virus RNA-dependent RNA polymerase: role for G3BP1 and G3BP2 in virus replication. J. Virol. **84**:6720–6732.

12. **Frolova E, Gorchakov R, Garmashova N, Atasheva S, Vergara LA, Frolov I.** 2006. Formation of nsP3-specific protein complexes during Sindbis virus replication. J. Virol. **80**:4122–4134.

13. **Frolova EI, Gorchakov R, Pereboeva L, Atasheva S, Frolov I.** 2010. Functional Sindbis virus replicative complexes are formed at the plasma membrane. J. Virol. **84**:11679–11695.

14. **Gorchakov R, Garmashova N, Frolova E, Frolov I.** 2008. Different types of nsP3-containing protein complexes in Sindbis virus-infected cells. J. Virol. **82**:10088–10101.

15. **Jose J, Snyder JE, Kuhn RJ.** 2009. A structural and functional perspective of alphavirus replication and assembly. Future Microbiol. **4**:837–856.

16. **Sawicki DL, Barkhimer DB, Sawicki SG, Rice CM, Schlesinger S.** 1990. Temperature sensitive shut-off of alphavirus minus strand RNA synthesis maps to a nonstructural protein, nsP4. Virology **174**:43–52.

17. **Shirako Y, Strauss JH.** 1990. Cleavage between nsP1 and nsP2 initiates the processing pathway of Sindbis virus nonstructural polyprotein P123. Virology **177**:54–64.

18. **Shirako Y, Strauss JH.** 1994. Regulation of Sindbis virus RNA replication: uncleaved P123 and nsP4 function in minus-strand RNA synthesis, whereas cleaved products from P123 are required for efficient plus-strand RNA synthesis. J. Virol. **68**:1874–1885.

19. **Ahola T, Laakkonen P, Vihinen H, Kaariainen L.** 1997. Critical residues of Semliki Forest virus RNA capping enzyme involved in methyltransferase and guanylyltransferase-like activities. J. Virol. **71**:392–397.

20. **Gomez de Cedron M, Ehsani N, Mikkola ML, Garcia JA, Kaariainen L.** 1999. RNA helicase activity of Semliki Forest virus replicase protein NSP2. FEBS Lett. **448**:19–22.

21. **Rikkonen M.** 1996. Functional significance of the nuclear-targeting and NTP-binding motifs of Semliki Forest virus nonstructural protein nsP2. Virology **218**:352–361.

22. **Rikkonen M, Peranen J, Kaariainen L.** 1994. ATPase and GTPase activities associated with Semliki Forest virus nonstructural protein nsP2. J. Virol. **68**:5804–5810.

23. **Vasiljeva L, Merits A, Auvinen P, Kaariainen L.** 2000. Identification of a novel function of the alphavirus capping apparatus. RNA 5′-triphosphatase activity of Nsp2. J. Biol. Chem. **275**:17281–17287.

24. **Lemm JA, Rice CM.** 1993. Roles of nonstructural polyproteins and cleav-

25. **Lemm JA, Rümenapf T, Strauss EG, Strauss JH, Rice CM.** 1994. Polypeptide requirements for assembly of functional Sindbis virus replication complexes: a model for the temporal regulation of minus and plus-strand RNA synthesis. EMBO J. **13**:2925–2934.

26. **Russo AT, White MA, Watowich SJ.** 2006. The crystal structure of the Venezuelan equine encephalitis alphavirus nsP2 protease. Structure **14**:1449–1458.

27. **Li ML, Stollar V.** 2007. Distinct sites on the Sindbis virus RNA-dependent RNA polymerase for binding to the promoters for the synthesis of genomic and subgenomic RNA. J. Virol. **81**:4371–4373.

28. **Li ML, Stollar V.** 2004. Identification of the amino acid sequence in Sindbis virus nsP4 that binds to the promoter for the synthesis of the subgenomic RNA. Proc. Natl. Acad. Sci. U. S. A. **101**:9429–9434.

29. **De I, Fata-Hartley C, Sawicki SG, Sawicki DL.** 2003. Functional analysis of nsP3 phosphoprotein mutants of Sindbis virus. J. Virol. **77**:13106–13116.

30. **LaStarza MW, Lemm JA, Rice CM.** 1994. Genetic analysis of the nsP3 region of Sindbis virus: evidence for roles in minus-strand and subgenomic RNA synthesis. J. Virol. **68**:5781–5791.

31. **LaStarza MW, Grakoui A, Rice CM.** 1994. Deletion and duplication mutations in the C-terminal nonconserved region of Sindbis virus: effects on phosphorylation and on virus replication in vertebrate and invertebrate cells. Virology **202**:224–232.

32. **Peranen P.** 1991. Localization and phosphorylation of Semliki Forest virus non-structural protein nsP3 expressed in COS cells from a cloned cDNA. J. Gen. Virol. **72**(Part 1):195–199.

33. **Malet H, Coutard B, Jamal S, Dutartre H, Papageorgiou N, Neuvonen M, Ahola T, Forrester N, Gould EA, Lafitte D, Ferron F, Lescar J, Gorbalenya AE, de Lamballerie X, Canard B.** 2009. The crystal structures of Chikungunya and Venezuelan equine encephalitis virus nsP3 macro domains define a conserved adenosine binding pocket. J. Virol. **83**:6534–6545.

34. **Shin G, Yost SA, Miller MT, Elrod EJ, Grakoui A, Marcotrigiano J.** 2012. Structural and functional insights into alphavirus polyprotein processing and pathogenesis. Proc. Natl. Acad. Sci. U. S. A. **109**:16534–16539.

35. **Rungrotmongkol T, Nunthaboot N, Malaisree M, Kaiyawet N, Yotmanee P, Meeprasert A, Hannongbua S.** 2010. Molecular insight into the specific binding of ADP-ribose to the nsP3 macro domains of chikungunya and Venezuelan equine encephalitis viruses: molecular dynamics simulations and free energy calculations. J. Mol. Graph. Model. **29**:347–353.

36. **Lulla A, Lulla V, Merits A.** 2012. Macromolecular assembly-driven processing of the 2/3 cleavage site in the alphavirus replicase polyprotein. J. Virol. **86**:553–565.

37. **Atasheva S, Krendelchtchikova V, Liopo A, Frolova E, Frolov I.** 2010. Interplay of acute and persistent infections caused by Venezuelan equine encephalitis virus encoding mutated capsid protein. J. Virol. **84**:10004–10015.

38. **Rice CM, Levis R, Strauss JH, Huang HV.** 1987. Production of infectious RNA transcripts from Sindbis virus cDNA clones: mapping of lethal mutations, rescue of a temperature-sensitive marker, and *in vitro* mutagenesis to generate defined mutants. J. Virol. **61**:3809–3819.

39. **Liljeström P, Lusa S, Huylebroeck D, Garoff H.** 1991. *In vitro* mutagenesis of a full-length cDNA clone of Semliki Forest virus: the small 6,000-molecular-weight membrane protein modulates virus release. J. Virol. **65**:4107–4113.

40. **Lemm JA, Durbin RK, Stollar V, Rice CM.** 1990. Mutations which alter the level or structure of nsP4 can affect the efficiency of Sindbis virus replication in a host-dependent manner. J. Virol. **64**:3001–3011.

41. **Foy NJ, Akhrymuk M, Akhrymuk I, Atasheva S, Bopda-Waffo A, Frolov I, Frolova EI.** 2013. Hypervariable domains of nsP3 proteins of New World and Old World alphaviruses mediate formation of distinct, virus-specific protein complexes. J. Virol. **87**:1997–2010.

42. **Vihinen H, Ahola T, Tuittila M, Merits A, Kaariainen L.** 2001. Elimination of phosphorylation sites of Semliki Forest virus replicase protein nsP3. J. Biol. Chem. **276**:5745–5752.

43. **Vihinen H, Saarinen J.** 2000. Phosphorylation site analysis of Semliki Forest virus nonstructural protein 3. J. Biol. Chem. **275**:27775–27783.

44. **Frolov I, Agapov E, Hoffman TA, Jr, Prágai BM, Lippa M, Schlesinger S, Rice CM.** 1999. Selection of RNA replicons capable of persistent noncytopathic replication in mammalian cells. J. Virol. **73**:3854–3865.

45. **Frolova EI, Fayzulin RZ, Cook SH, Griffin DE, Rice CM, Frolov I.** 2002.

Roles of nonstructural protein nsP2 and alpha/beta interferons in determining the outcome of Sindbis virus infection. J. Virol. **76**:11254–11264.

46. **Gorchakov R, Frolova E, Frolov I.** 2005. Inhibition of transcription and translation in Sindbis virus-infected cells. J. Virol. **79**:9397–9409.

47. **Atasheva S, Kim DY, Akhrymuk M, Morgan DG, Frolova EI, Frolov I.** 2013. Pseudoinfectious Venezuelan equine encephalitis virus: a new means of alphavirus attenuation. J. Virol. **87**:2023–2035.

48. **Kim DY, Atasheva S, Frolova EI, Frolov I.** 2013. Venezuelan equine encephalitis virus nsP2 protein regulates packaging of the viral genome into infectious virions. J. Virol. **87**:4202–4213.

49. **Galbraith SE, Sheahan BJ, Atkins GJ.** 2006. Deletions in the hypervariable domain of the nsP3 gene attenuate Semliki Forest virus virulence. J. Gen. Virol. **87**:937–947.

50. **Akhrymuk I, Kulemzin SV, Frolova EI.** 2012. Evasion of the innate immune response: the Old World alphavirus nsP2 protein induces rapid degradation of Rpb1, a catalytic subunit of RNA polymerase II. J. Virol. **86**:7180–7191.

51. **Ding MX, Schlesinger MJ.** 1989. Evidence that Sindbis virus NSP2 is an autoprotease which processes the virus nonstructural polyprotein. Virology **171**:280–284.

52. **Garmashova N, Gorchakov R, Volkova E, Paessler S, Frolova E, Frolov I.** 2007. The Old World and New World alphaviruses use different virus-specific proteins for induction of transcriptional shutoff. J. Virol. **81**:2472–2484.

53. **Karpe YA, Aher PP, Lole KS.** 2011. NTPase and 5′-RNA triphosphatase activities of Chikungunya virus nsP2 protein. PLoS One **6**:e22336. doi:10.1371/journal.pone.0022336.

54. **Lampio A, Kilpelainen I, Pesonen S, Karhi K, Auvinen P, Somerharju P, Kaariainen L.** 2000. Membrane binding mechanism of an RNA virus-capping enzyme. J. Biol. Chem. **275**:37853–37859.

55. **Rubach JK, Wasik BR, Rupp JC, Kuhn RJ, Hardy RW, Smith JL.** 2009. Characterization of purified Sindbis virus nsP4 RNA-dependent RNA polymerase activity in vitro. Virology **384**:201–208.

56. **Rupp JC, Jundt N, Hardy RW.** 2011. Requirement for the amino-terminal domain of Sindbis virus nsP4 during virus infection. J. Virol. **85**:3449–3460.

57. **Russo AT, Malmstrom RD, White MA, Watowich SJ.** 2010. Structural basis for substrate specificity of alphavirus nsP2 proteases. J. Mol. Graph. Model. **29**:46–53.

58. **Sawicki DL, Perri S, Polo JM, Sawicki SG.** 2006. Role for nsP2 proteins in the cessation of alphavirus minus-strand synthesis by host cells. J. Virol. **80**:360–371.

59. **Spuul P, Salonen A, Merits A, Jokitalo E, Kaariainen L, Ahola T.** 2007. Role of the amphipathic peptide of Semliki forest virus replicase protein nsP1 in membrane association and virus replication. J. Virol. **81**:872–883.

60. **Tomar S, Narwal M, Harms E, Smith JL, Kuhn RJ.** 2011. Heterologous production, purification and characterization of enzymatically active Sindbis virus nonstructural protein nsP1. Protein Expr. Purif. **79**:277–284.

61. **Vasiljeva L, Valmu L, Kaariainen L, Merits A.** 2001. Site-specific protease activity of the carboxyl-terminal domain of Semliki Forest virus replicase protein nsP2. J. Biol. Chem. **276**:30786–30793.

62. **Zhang D, Tozser J, Waugh DS.** 2009. Molecular cloning, overproduction, purification and biochemical characterization of the p39 nsp2 protease domains encoded by three alphaviruses. Protein Expr. Purif. **64**:89–97.

63. **Fros JJ, Domeradzka NE, Baggen J, Geertsema C, Flipse J, Vlak JM, Pijlman GP.** 2012. Chikungunya virus nsP3 blocks stress granule assembly by recruitment of G3BP into cytoplasmic foci. J. Virol. **86**:10873–10879.

64. **Garmashova N, Gorchakov R, Frolova E, Frolov I.** 2006. Sindbis virus nonstructural protein nsP2 is cytotoxic and inhibits cellular transcription. J. Virol. **80**:5686–5696.

65. **Neuvonen M, Kazlauskas A, Martikainen M, Hinkkanen A, Ahola T, Saksela K.** 2011. SH3 domain-mediated recruitment of host cell amphiphysins by alphavirus nsP3 promotes viral RNA replication. PLoS Pathog. **7**:e1002383. doi:10.1371/journal.ppat.1002383.

66. **Tuittila M, Hinkkanen AE.** 2003. Amino acid mutations in the replicase protein nsP3 of Semliki Forest virus cumulatively affect neurovirulence. J. Gen. Virol. **84**:1525–1533.

67. **Panas MD, Varjak M, Lulla A, Eng KE, Merits A, Karlsson Hedestam GB, McInerney GM.** 2012. Sequestration of G3BP coupled with efficient translation inhibits stress granules in Semliki Forest virus infection. Mol. Biol. Cell **23**:4701–4712.

68. **Park E, Griffin DE.** 2009. The nsP3 macro domain is important for Sindbis virus replication in neurons and neurovirulence in mice. Virology **388**:305–314.

69. **Aaskov J, Jones A, Choi W, Lowry K, Stewart E.** 2011. Lineage replacement accompanying duplication and rapid fixation of an RNA element in the nsP3 gene in a species of alphavirus. Virology **410**:353–359.

70. **Davis NL, Willis LV, Smith JF, Johnston RE.** 1989. In vitro synthesis of infectious Venezuelan equine encephalitis virus RNA from a cDNA clone: analysis of a viable deletion mutant. Virology **171**:189–204.